The Three-Dimensional Localization of Internal Mammary Lymph Nodes by Radionuclide Lymphoscintigraphy

William D. Kaplan, Janet W. Andersen, Robert L. Siddon, Barbara T. Connolly, Carol A. McCormick, Susan M. Laffin, Eileen M. Rosenbaum, Clare A. Jennings, Abram Recht, and Jay R. Harris

Joint Program in Nuclear Medicine and Joint Center for Radiation Therapy, Harvard Medical School and the Departments of Radiology and Biostatistics, Dana-Farber Cancer Institute, Boston, Massachusetts

In breast cancer patients, radiation therapy planning must account for individual anatomy to ensure optimal coverage of tumor and internal mammary nodes. To achieve this, three-dimensional radionuclide lymphoscintigraphy (RNLS) was performed in 167 patients by obtaining two images of the nodes using a 30-degree slant hole collimator rotated 180° between images. Analysis of 768 nodes (mean 4.6/patient) visualized from the level of rib 1 through interspace 5 was performed. The number of nodes seen was not a function of patient age. Cross-communication to the contralateral node chain occurred in 13.8% of cases. Eighty-two percent of nodes were located near the first three ribs and interspaces; 23% were located beyond 3.0 cm from the mid-sternal line. At the level of the radiation beam match line (second rib or interspace), 4.5% of nodes were deeper than 3.0 cm. From rib 3 through interspace 5, 3.9% were deeper than 3.0 cm. Using an idealized tangential field, at least one node would have been missed in 16.2% of patients. Three-dimensional RNLS allows definition and localization of normal sized nodes and ensures that radiation therapy portals can be tailored for each individual under treatment.

J Nucl Med 29:473–478, 1988

The internal mammary lymph node chain originates at the level of the sixth intercostal space, receives afferent lymph channels from the diaphragm and liver, and terminates behind the sternal head of the sternocleidomastoid muscle. The main efferent breast lymphatics to this chain emerge from the nipple region and both the deep and medial edges of the breast. These channels either lie upon the pectoral fascia or pierce it to enter the pectoralis major muscle, accompanying branches of the perforating blood vessels to reach the medial aspect of the intercostal spaces. Here, usually at a point just above the costal cartilage of each rib, the lymphatic bundles turn inward, penetrate the muscles and empty into the internal mammary nodes.

In anatomic series, these nodes occur with greatest frequency in the second, first, and third interspaces, in that order (*1*). However, they vary from one patient to another in both position and number and in many cases may be recognizable only by microscopic evaluation (*2,3*).

On the basis of measurements made at autopsy, radiation therapy planning has assumed these nodes to be located no more than 3 cm deep and 3 cm lateral to the midline (*3–5*). However, accurate premortem knowledge of their precise location would not only ensure optimal coverage during external beam radiation therapy but could also allow for a reduction in exposure of normal tissue when lymph nodes are positioned superficially and close to midline.

Standard radiographic techniques for identifying and localizing these nodes in three-dimensional space have been disappointing. Results of a computerized tomographic (CT) study by Munzenrider et al. showed that in a population of 46 postmastectomy patients, normal internal mammary lymph nodes could not be routinely visualized (*6*). On the other hand, Ege showed that routine localization of these nodes was possible using RNLS (*7*) while Collier et al. (*8*) in comparative study

Received Feb. 5, 1987; revision accepted Sept. 10, 1987.

For reprints contact: William D. Kaplan, MD, Dana-Farber Cancer Institute, Div. of Nuclear Medicine, 44 Binney St., Boston, MA 02115.

of these two radiographic techniques showed that lymphoscintigraphy was the method of choice for delineating internal mammary nodal structures and associated lymphatic drainage routes. They indicated that the radionuclide approach was preferable for identifying 2–4 mm normally functioning nodes since the size limit of CT identification was on the order of 7 to 8 mm (*9*). A report on the combined use of RNLS and plain radiographic reconstruction of patient surface anatomy to more accurately deliver electron beam therapy underscored the utility of the nuclear medicine technique in these patients (*10*). The present study was undertaken to document the number and anatomic location of these nodes and to relate these findings to important technical considerations associated with radiation therapy planning in patients with carcinoma of the breast.

MATERIALS AND METHODS

The results of lymphoscintigraphic studies of 167 consecutive patients were analyzed. Only patient scans which showed a pattern of normal uptake were included in the evaluation. (At our hospital, ~95% of lymphoscintigraphic studies are normal.) A normal pattern showed the full extent of the lymphatic chain, presence of discrete intranodal radiocolloid aggregation, and a similar intensity of radiocolloid uptake within nodes from the level of the xyphoid to the manubrium.

Since, in our institution, the primary reason for performing RNLS is to design optimal opposing beam radiation therapy portals to treat nodes at greatest risk for metastasis, only those nodes located between the first rib and the fifth intercostal space (*11*), were considered in the final three-dimensional analysis.

Study Parameters

Injection technique. The anatomic site and technique for radiocolloid administration have been previously described (*7*). We injected between 0.5 and 1.0 mCi of technetium-99m (^{99m}Tc) antimony trisulfide colloid (Sb_2S_3) (Cadema Medical Products Inc., Middletown, NY) in a volume of between 0.1 and 0.2 ml. The patients were in a supine position for the injection which was administered at a point ~3 cm inferior to the xyphoid process and 1–2 cm medial to the mid-clavicular line on the side under evaluation. A 1.0-ml tuberculin syringe, fitted with a 22 gauge, 1½-in. needle was used. The depth of the injection was controlled by applying tension to the skin and underlying rectus muscle with the free hand. The radiocolloid was deposited at a depth of ~2 cm, just anterior to the posterior rectus sheath.

Imaging. Imaging was performed on a Siemens, 37 photomultiplier tube, low energy, mobile gamma camera. Image collection began 3 hr after injection with the patient positioned supinely for all views. For parallel hole collimation, a low-energy, all-purpose collimator was used. An anterior 100,000 count image was accumulated over the thorax. Included within the field of view were the sternal notch, delineated by a cobalt-57 (^{57}Co) disk marker, and the most superior aspect of the injection site.

Additional 100,000 count parallel hole views included: (a) an anterior view of the thorax with three ^{57}Co markers positioned at the sternal notch, mid sternum, and xyphisternum, respectively, to define the midline of the chest (Fig. 1); and (b) an anterior view of the thorax with a series of radioactive markers defining the costochondral junction of the first five ribs. This latter view was compared with a chest x-ray (obtained with lead markers positioned over the first three ribs) to ensure that the ribs identified on the scan were accurately identified.

Three-dimensional imaging. The technique described by Siddon et al. (*12*) was used to obtain stereolymphoscintigraphic images. With ^{57}Co markers placed on the patient's sternal notch, mid-sternum, and xyphisternum, a rotating 30-degree slant hole collimator (Engineering Dynamics Corporation, Lowell, MA) was positioned horizontally above the patient. The field of view included all the internal mammary lymph nodes and the three ^{57}Co markers. Two 100,000 count images were then obtained with the collimator rotated 180° between images (Fig. 1). The patient remained in a fixed position throughout the procedure.

Three-dimensional analysis. All imaging data were analyzed on a system consisting of (a) a VAX 11/785 computer, (b) Summagraphics digitizing tablet, and (c) a LEXIDATA 3400 image display station. All computer code was written in FORTRAN-77, and run under the VMS operating system.

Output from the gamma camera was in the form of 3″ × 5″ black and white polaroid prints. Distance scaling from the photographic print to the digitizer tablet was provided by an image obtained with four ^{57}Co markers placed at the corners of a 10-cm square.

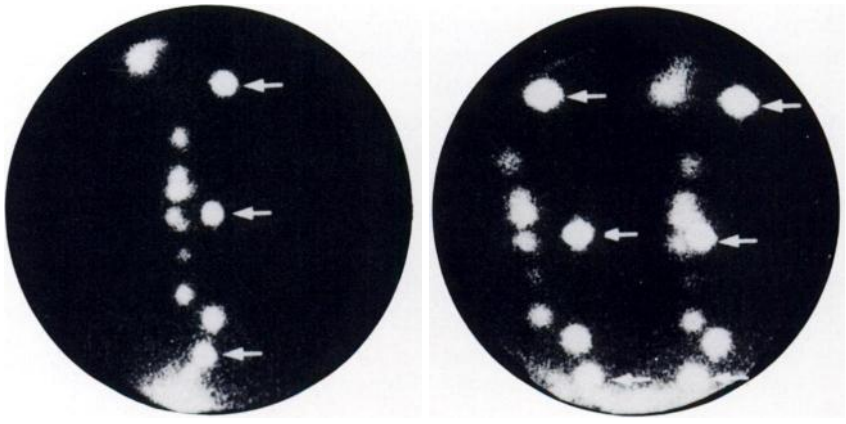

FIGURE 1
Anterior, parallel hole collimator view of a normal RNLS (left). Cobalt-57 markers at the sternal notch, mid sternum and xyphoid are indicated by arrows. An anterior, double-exposure, 30-degree slant hole collimator view of the same patient (right) shows the paired nodes and ^{57}Co markers (arrows).

All parasternal lymph node images were digitized and the three-dimensional coordinates were obtained (*12*). Briefly, for a given pair of images, the position of the radioactive point source (^{57}Co marker or lymph node) in the plane of the camera is at the mid-point of a straight line connecting the two foci. The distance of the object from the camera (depth) is then given by R/tanΘ, where R is one-half the distance between the two paired foci and Θ is the angle of the slant holes (30°).

Statistical methods. Data were analyzed using the ANOVA, one-way analysis of variance.

RESULTS

Number of Nodes Seen

A total of 1,020 lymph nodes were identified between the xyphisternum and the sternal notch in the 167 patients studied (mean = 6.1 nodes/patient). From the level of the first rib through the fifth intercostal space, 768 nodes were identified (mean = 4.6 nodes/patient) and analyzed.

Relationship to Age

To determine the relationship between age and number of lymph nodes visualized, patients were grouped into (a) those <40 yr (median age 36; number of cases 34), (b) those between 40 and 49 yr (median age 46; number of cases 43), (c) those from 50 to 59 yr (median age 55; number of cases 44), and (d) those older than 60 yr of age (median age 69; number of cases 46). The F-ratio which compares the mean number of nodes in each group was 0.559, giving a p-value of 0.643. This indicated that there was no significant difference in the mean number of nodes visualized as a function of patient age (Table 1).

Level of Cross-Drainage

We noted cross-drainage of lymph nodes to the contralateral side in 23 of the 167 patients (13.8%). In 13 of the 23 (56.5%), this occurred at the sternomanubrial junction, the most frequent site. The xyphisternum was the next most frequent, noted in six of the 23 patients (26.1%), with the mid sternum the least common site for cross drainage, noted in only four or 17.4% of patients (Table 2).

TABLE 1
Visualization of 768 Nodes* as a Function of Age (yr)

Age (yr)	Median	No. cases	No. mammary nodes Mean	Median	s.d.
<4	36	34	4.6	4.0	1.6
40–49	46	43	4.5	4.5	1.8
50–59	55	44	4.8	5.0	1.9
>60	69	46	4.6	4.0	2.0

* Rib 1 through interspace 5.

TABLE 2
Location of Cross Drainage of Internal Mammary Nodes in 23 Patients Following Subcostal Radiocolloid Injection

Location	Number	Percent
Sternomanubrial jct*	13/23	56.5
Xyphoid	6/23	26.1
Midsternum	4/23	17.4

* Jct = junction.

Spatial Distribution

Location by rib/interspace. When the location of each of the 768 lymph nodes was defined, we found that 82% of the nodes were localized to the first three ribs and interspaces. The largest percentage of nodes was seen in the second rib/interspace (35.5%), with the first (24.8%) and third (21.7%) rib/interspace locations noted to contain the next greatest percentage of nodes, in that order (Table 3). Decreasingly fewer nodes were noted at the levels of the midsternum and xyphisternum (Table 3, Fig. 2).

When location was plotted as a function of distance from the midline in the anterior-posterior projection, it was noted that 23% of nodes were positioned more than 3 cm from the mid sternal line and that the internal mammary lymphatic chains deviated laterally at their more cephalad location (Table 4, Fig. 2).

When lymph node depth was plotted as a function of rib and interspace level, we found that the nodes at the xyphisternum were more superficial with deeper substernal locations assumed by the more cephalad nodes. At the level of the match line between the tangential and en-face radiation therapy beams (second rib or second interspace), there were 35/768 nodes (4.5%) at a depth >3.0 cm whereas from the third rib through the fifth interspace, a total of 30 nodes (3.9%) were positioned at a depth >3.0 cm (Table 5, Fig. 3).

Radiation Portal Coverage

The idealized tangential field assumes inclusion of all lymph nodes located in interspaces two through five and also assumes that the radiation beam enters the

TABLE 3
Distribution of 768 Internal Mammary Lymph Nodes by Rib (R) and Interspace (I) in 167 Patients

Site	No.	Percent
R 1	56	7.6
I 1	132	17.2
R 2	144	18.8
I 2	128	16.7
R 3	93	12.1
I 3	74	9.6
R 4	49	6.4
I 4	35	4.5
R 5	36	4.7
I 5	21	2.7

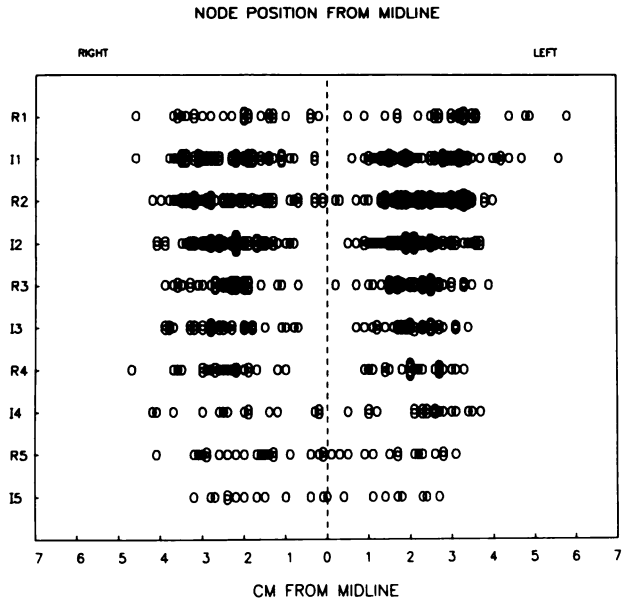

FIGURE 2
Computer plot of 768 lymph nodes superimposed on an anterior thorax to define nodal position with respect to midline, ribs (R) and interspaces (I).

thorax 3 cm contralateral to midline and anterior to a 35-degree plane. Based upon these assumptions, we found that 37 of 768 nodes (4.8%) would have been outside the field with this treatment plan. These 37 lymph nodes represented 27 of the 167 patients (16.2%) evaluated.

DISCUSSION

Treatment of the internal mammary nodes in patients with breast cancer has been controversial; although such treatment is associated with improved local tumor control, most studies have failed to show improved survival. It has been suggested that patients with pathologically positive axillary nodes or inner quadrant or central lesions may benefit from this therapy (*13*, *14*). We feel that irradiation of the internal mammary nodes is justified if there is both a significant risk of their involvement, and if the toxicity of such treatment is small. This implies that the additional lung and/or heart volume included in the radiation field is minimized. Therefore, in the individualized treatment of primary breast cancer, it may be important to know chest wall thickness and, ideally, the specific location of each internal mammary lymph node. Although the former can be determined by CT, internal mammary nodes are not routinely visualized during CT imaging for radiation treatment planning procedures (*6*). Ultrasound techniques, designed to determine the depth of the internal mammary lymph node chain, do not routinely visualize discrete nodes and therefore must rely upon measurements of the distance between the skin surface and the pleura to "localize" these lymphatic structures (*15*).

There is excellent correlation between the number of internal mammary nodes seen by RNLS techniques and the number as defined by careful postmortem examinations. In a survey of 60 patients, Stibbe (*1*), found the average total number of internal mammary lymph nodes to be 8.5. In 39 autopsies, Soerensen found an average of seven nodes per subject (*16*). In a series of 100 autopsies, Ju (*17*), found an average of 6.2 nodes per subject and Putti (*18*) in an evaluation of the number and arrangement of internal mammary nodes in 47 cadavers, found an average of 7.7 lymph nodes per subject. These findings are similar to the mean

TABLE 4
Number of Nodes (%) Greater than Given Distance from Midline by RIB (R) and Interspace (I)

Location	Distance in cm				
	>2.0	>2.5	>3.0	>3.5	>4.0
R 1 (n* = 56)	36 (64)	32 (57)	24 (42)	11 (20)	5 (9)
I 1 (n = 132)	80 (61)	66 (50)	39 (30)	12 (9)	7 (5)
R 2 (n = 144)	92 (64)	66 (46)	44 (30)	8 (6)	1 (1)
I 2 (n = 128)	78 (61)	46 (36)	22 (17)	8 (6)	2 (2)
R 3 (n = 93)	58 (62)	26 (28)	13 (14)	5 (5)	0
I 3 (n = 74)	43 (58)	28 (38)	14 (19)	6 (8)	0
R 4 (n = 49)	30 (61)	21 (43)	6 (12)	3 (6)	1 (2)
I 4 (n = 35)	23 (66)	15 (43)	7 (20)	4 (11)	2 (6)
R 5 (n = 36)	16 (44)	11 (30)	4 (11)	1 (3)	1 (3)
I 5 (n = 21)	9 (43)	4 (19)	1 (5)	0	0
Total nodes (n = 768)	465 (60)	315 (41)	174 (23)	58 (8)	19 (2)
Patients (n = 167) with any nodes	156 (93)	138 (41)	106 (63)	37 (22)	13 (8)

*Number.

TABLE 5
Depth (cm) of 768 Nodes as Related to RIB (R) and Interspace (I)

	Location										
Depth	R1	I1	R2	I2	R3	I3	R4	I4	R5	I5	Total
0.1–0.5	1	3	3	4	0	2	0	0	0	0	13
0.6–1.0	1	9	17	19	15	6	3	1	0	3	74
1.1–1.5	3	22	36	23	25	19	11	6	5	4	154
1.6–2.0	6	20	37	36	19	18	17	8	9	3	173
2.1–2.5	11	21	20	19	16	16	12	8	9	5	137
2.6–3.0	14	23	11	12	9	9	4	7	6	3	98
3.1–3.5	4	12	5	7	3	1	1	4	3	3	43
3.6–4.0	9	11	6	2	1	2	0	1	3	0	35
4.1–4.5	5	4	4	3	4	1	0	0	0	0	21
4.6–5.0	1	3	4	0	1	0	1	0	1	0	11
5.1–5.5	1	1	0	2	0	0	0	0	0	0	4
5.6–6.0	0	2	0	1	0	0	0	0	0	0	3
6.1–6.5	0	0	0	0	0	0	0	0	0	0	0
6.6–7.0	0	1	1	0	0	0	0	0	0	0	2
Total	56	132	144	128	93	74	49	35	36	21	768

number of 6.1 nodes/patient identified by RNLS in our study.

There has been a suggestion in the literature that the parasternal lymph nodes may show a decrease in phagocytic function with age (*1*). Although Ege was unable to document a lesser number of visualized nodes in older patients (*7*), she did suggest that there may be some decrease in reticuloendothelial activity, manifested as a decrease in relative radiocolloid nodal uptake. Our analysis showed no statistically significant difference in the number of nodes visualized as a function of patient age.

Although RNLS may not be capable of identifying microscopic foci of lymphoid tissue devoid of reticuloendothelial elements, CT scanning is not without potential pitfalls in the definition of nodes. These include: (a) overestimating the total number of lymph nodes by failing to distinguish them from regional blood vessels and (b) underestimating the number because of the need to have a 7-mm diameter node before identification is reliable (*8*).

In terms of rib and interspace distribution, our scintigraphic findings correlate well with the CT findings of Meyer et al. (*9*) who noted that 83% of the enlarged nodes seen with internal mammary nodal adenopathy occurred in the first and second intercostal spaces at the level of the manubrium and proximal sternal body. In our study, 82% of the 768 nodes identified were located at approximately these levels. We could also confirm that the nodes are deeper to the sternum at their more cephalad position (Table 5), a finding alluded to by both Bernardino (*15*) and Ragnhult (*19*).

The position of the internal mammary nodes can vary so much that radiation therapy planning, which assumes a "fixed and known" anatomic location for these structures, can in reality be inaccurate. Ege (*7*) showed that the anterior-posterior relationship of these nodes to the sternal border or midsternal line was anywhere from 3 to 5 cm off the midline. Similarly, Rose et al. (*20*) found that a significant number of patients treated by tangential portals using the arbitrary rule that all nodes were within 3.0 cm deep and lateral to midline had at least one internal mammary node inadequately treated. Our results in this larger series, using a more accurate method of three dimensional localization, corroborate and underscore these findings.

Three-dimensional RNLS both defines and localizes normal-sized nodes and documents the variability in nodal position from patient to patient. With this knowledge, radiation therapy portals need not be based on an idealized model but rather can be specifically tailored for each individual under treatment, thereby ensuring delivery of therapy to nodes at risk for metastatic deposits and the sparing of normal lung and cardiac tissue in patients with superficial and medial lymphatic structures.

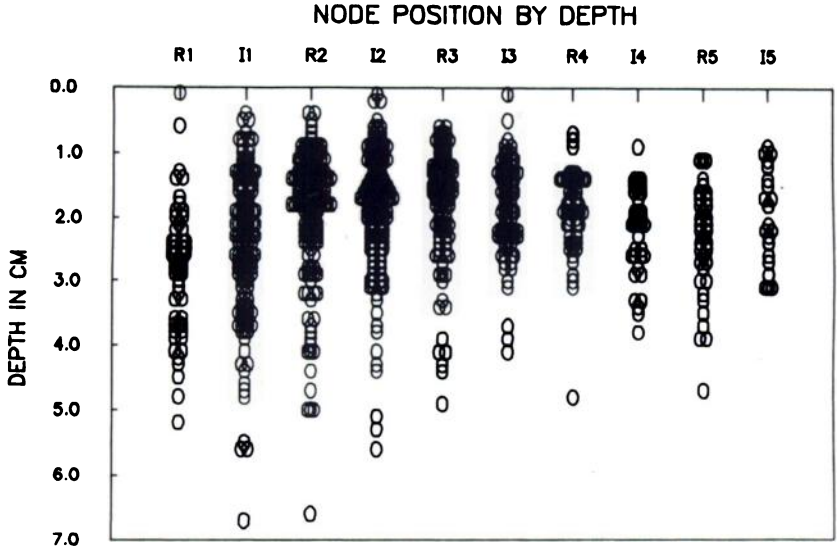

FIGURE 3
Computer plot of 768 lymph nodes superimposed on the right lateral thorax of an idealized supine patient (head positioned at left). Node position is defined with respect to depth (cm) from skin surface over sternum and location with respect to ribs (R) and interspaces (I).

ACKNOWLEDGMENTS

The authors thank Jeffrey Stoia for her editorial comments and suggestions, John Buckley for photography and Laurie Pugsley for her tireless assistance in the preparation of the manuscript.

REFERENCES

1. Stibbe EP. The internal mammary lymphatic glands. *J Anat* 1918; 52:257–264.
2. Handley RS, Thackray AC. Invasion of internal mammary lymph nodes in carcinoma of the breast. *Br Med J* 1954; 1:61–63.
3. Haagensen CD. Lymphatics of the breast. In: Haagensen CD, Feind CR, Herter FP, Slanetz CA, Weinberg JA, eds. *The lymphatics in cancer.* Philadelphia: W. B. Saunders Co, 1972:300–398.
4. Fletcher GT, Tapley N du V, Montague ED, Brown GR. Management of localized breast cancer. In: *Textbook of radiotherapy.* Philadelphia: Lea and Febiger, 1973:457–493.
5. Lindskoug B, Hultborn A. Tissue heterogeneity in the anterior chest wall and its influence on radiation therapy of the internal mammary lymph nodes. *Acta Radiol Ther* 1976; 15:97–116.
6. Munzenrider JE, Tchakavora I, Castro M, et al. Computerized body tomography in breast cancer. *Cancer* 1979; 43:137–150.
7. Ege G. Internal mammary lymphoscintigraphy. *Radiology* 1976; 118:101–107.
8. Collier BD, Palmer DW, Wilson JF, et al. Internal mammary lymphoscintigraphy in patients with breast cancer. *Radiology* 1983; 147:845–848.
9. Meyer JE, Munzenrider JE. Computed tomographic demonstration of internal mammary lymph node metastasis in patients with locally recurrent breast carcinoma. *Radiology* 1981; 139:661–663.
10. Jones D, Hanelin L, Christopherson D, et al. Radiotherapy treatment planning using lymphoscintigraphy. *Int J Radiat Oncol Biol Phys* 1986; 12:1707–1710.
11. Urban JA, Marjani MA. Significance of internal mammary lymph node metastasis in breast cancer. *Am J Roentgenol* 1971; 111:130–136.
12. Siddon RL, Chin LM, Zimmerman RE, et al. Utilization of parasternal lymphoscintigraphy in radiation therapy of breast carcinoma. *Int J Radiat Oncol Biol Phys* 1982; 8:1059–1063.
13. Host H, Brennhovd IO, Loeb M. Postoperative radiotherapy in breast cancer—long-term results from the Oslo study. *Int J Radiat Oncol Biol Phys* 1985; 12:727–732.
14. Wallgren A, Arner O, Bergstrom J, et al. Radiation therapy in operable breast cancer: results from the Stockholm trial on adjuvant radiotherapy. *J Radiat Oncol Biol Phys* 1985; 12:533–537.
15. Bernardino ME, Spanos Jr W. A simple technique for determining internal mammary chain depth by sonography. *Int J Radiat Oncol Biol Phys* 1981; 7:671–673.
16. Soerensen B. Recherches sur la localisation des ganglions lymphatiques parasternaux par rapport aux espaces intercostaux. *Internat J Chir* 1951; 11:501–509.
17. Ju D. Lymphatics of the breast. In: Haagensen CD, Feind CR, Herter FP, Slanetz CA, Weinberg JA, eds. *The lymphatics in cancer.* Philadelphia: W. B. Saunders Co., 1972:300–398.
18. Putti F. Ricerche anatomiche sui linfonodi mammari interni. *Chirurgia Italiana* 1953; 7:161–167.
19. Ragnhult I, Lindskoug B, Hultborn A. Dosimetric investigation of post-operative irradiation of regional lymph nodes in mammary carcinoma. *Acta Radiol* 1972; 313(suppl):135–147.
20. Rose CM, Kaplan WD, Marck A, et al. Parasternal lymphoscintigraphy: Implications for the treatment planning of internal mammary lymph nodes in breast cancer. *Int J Radiat Oncol Biol Phys* 1979; 5:1849–1853.